OPEN

Dynamic Stabilization of Simple Fractures With Active Plates Delivers Stronger Healing Than Conventional Compression Plating

Michael Bottlang, PhD, Stanley Tsai, MS,* Emily K. Bliven, BS,* Brigitte von Rechenberg, DVM,† Philipp Kindt, DVM,† Peter Augat, PhD,‡§ Julia Henschel, BS,‡ Daniel C. Fitzpatrick, MD,‖ and Steven M. Madey, MD**

Objectives: Active plates dynamize a fracture by elastic suspension of screw holes within the plate. We hypothesized that dynamic stabilization with active plates delivers stronger healing relative to standard compression plating.

Methods: Twelve sheep were randomized to receive either a standard compression plate (CP) or an active plate (ACTIVE) for stabilization of an anatomically reduced tibial osteotomy. In the CP group, absolute stabilization was pursued by interfragmentary compression with 6 cortical screws. In the ACTIVE group, dynamic stabilization after bony apposition was achieved with 6 elastically suspended locking screws. Fracture healing was analyzed weekly on radiographs. After sacrifice 9 weeks postsurgery, the torsional strength of healed tibiae and contralateral tibiae was measured. Finally, computed tomography was used to assess fracture patterns and healing modes.

Results: Healing in both groups included periosteal callus formation. ACTIVE specimens had almost 6 times more callus area by week 9 ($P < 0.001$) than CP specimens. ACTIVE specimens recovered on average 64% of their native strength by week 9, and were over twice as strong as CP specimens, which recovered 24% of their native strength ($P = 0.008$). Microcomputed tomography demonstrated that compression plating induced a combination of primary bone healing and gap healing. Active plating consistently stimulated biological bone healing by periosteal callus formation.

Conclusions: Compared with compression plating, dynamic stabilization of simple fractures with active plates delivers significantly stronger healing.

Key Words: active plating, fracture healing, dynamization, compression plating, ovine

(*J Orthop Trauma* 2017;31:71–77)

INTRODUCTION

Over 5 decades of research on fracture healing provided consistent and abundant evidence that controlled dynamization of a fracture stimulates callus formation, resulting in faster and stronger healing relative to rigid fixation.[1–8] Conversely, overly rigid fixation with stiff plating constructs can suppress callus formation and biological bone healing, contributing to delayed union, nonunion, osteolysis, and fixation failure.[9–12]

The advent of locked plating enabled 2 new strategies for dynamization of fractures, namely screw dynamization with far cortical locking (FCL) screws,[13–17] and plate dynamization with active plates.[2,18,19] FCL screws lock into the plate and the far cortex, but retain a motion envelope at the near cortex. This enables controlled dynamization by flexion of the elastic shaft of FCL screws. In an ovine bridge plating model, FCL fixation led to circumferential callus bridging, and fractures healed to be twice as strong in torsion compared with standard locked plating.[1] For plate dynamization, active plates have screw holes that are integrated in individual sliding elements, which are elastically suspended in an elastomer envelope inside the plate.[19] This elastic suspension of screw holes allows controlled interfragmentary dynamization in addition to providing durable fixation of the active plate with standard locking screws. Dynamization with active plates stimulated early and circumferential callus formation after bridge plating of a 3-mm fracture gap in the ovine tibia.[2] Compared with standard locked plating, active plating specimens yielded over 6 times more callus by postoperative week 3, and healed to be 4 times stronger in torsion.[2]

Accepted for publication August 11, 2016.

From the *Portland Biomechanics Laboratory, Legacy Research Institute, Portland, OR; †Musculoskeletal Research Unit, Vetsuisse Faculty, University of Zürich, Zürich, Switzerland; ‡Institute of Biomechanics, Paracelsus Medical University, Salzburg, Austria; §Institute of Biomechanics, Trauma Center Murnau, Murnau, Germany; and ‖Slocum Center for Orthopedics and Sports Medicine, Eugene, OR.

This work has been funded in part by Zimmer Biomet, and by the National Institute of Health NIH/NIAMS Grant AP061201.

M. Bottlang, D. Fitzpatrick, and S. Madey receive royalties from Zimmer Biomet and serve on the Zimmer speaker bureau. The remaining authors report no conflict of interest.

Supplemental digital content is available for this article. Direct URL citations appear in the printed text and are provided in the HTML and PDF versions of this article on the journal's Web site (www.jorthotrauma.com).

Reprints: Michael Bottlang, PhD, Portland Biomechanics Laboratory, Legacy Research Institute, 1225 NE 2nd Avenue, Portland, OR 97232 (e-mail: mbottlan@lhs.org).

DOI: 10.1097/BOT.0000000000000732

These results demonstrated the benefits of active plating on bridging of a gap osteotomy representative of a comminuted fracture, in which controlled dynamization results in interfragmentary gap motion. However, the effect of active plating for dynamic stabilization of a simple, anatomically reduced fracture has not been investigated to date. The gold standard for plating of a simple diaphyseal fracture remains anatomic reduction and absolute stabilization. It uses compression plates (CPs) to target primary bone healing without callus formation. Interestingly, intramedullary nailing of the same simple diaphyseal fracture will seek functional reduction and relative stability to target secondary bone healing with callus formation. Callus is expected because the relative stability of an intramedullary nail permits sufficient dynamic loading at the fracture.

This controlled animal study evaluated the effect of dynamic stabilization with active plates on healing of a simple, anatomically reduced fracture. We hypothesize that compared with standard compression plating, dynamic stabilization of an anatomically reduced fracture with an active locking plate delivers stronger healing, as measured by the torsional strength of the healed fracture.

MATERIALS AND METHODS

Using an established large animal fracture healing model,[20] 12 sheep were randomly assigned to receive a standard CP or an active locking plate (ACTIVE) for stabilization of an anatomically reduced tibial osteotomy. In the CP group, absolute stability was achieved in accordance with compression plating principles.[21] In the ACTIVE group, dynamic stabilization was achieved with 6 locking screws, inserted in the elastically suspended locking holes of active plates after anatomic fracture reduction. Although the bone ends were abutting, no attempt was made to compress the ACTIVE plate group osteotomy. Beginning at postoperative week 3, fracture healing was assessed on bi-planar radiographs to measure callus size each week. After sacrifice 9 weeks postsurgery, healed tibiae and contralateral tibiae were tested in torsion until failure to determine their strength. Finally, computed tomography (CT) of tested tibiae was obtained to assess the fracture pattern, and micro-CT (μCT) was obtained to visualize healing modes.

Plating Constructs

Compression and ACTIVE plates had an identical cross-sectional geometry, representative of typical 4.5-mm large fragment plates. Plates had 6 holes, were 127 mm long, 16 mm wide, 5.6 mm thick, and were made of Ti6Al4V ELI titanium alloy. CPs had elongated screw holes with sloped shoulders to generate interfragmentary compression in response to eccentric screw placement (Fig. 1A). In strict adherence to compression plating principles,[21] mild overbending was applied to CPs to ensure symmetric interfragmentary compression. For ACTIVE plates, locking holes were integrated in individual sliding elements that were elastically suspended in a silicone envelope inside lateral plate pockets (Figs. 1B–D). The silicone suspension consisted of long-term implantable medical-grade silicone elastomer (HCRA 4750; Applied Silicone, Santa Paula, CA) that was molded onto the sliding elements. Lateral pockets were arranged in an alternating pattern from both plate sides, resulting in a staggered locking hole configuration. The stiffness and strength of ACTIVE plating constructs in the presence of normal and osteopenic bone have been evaluated previously in a comprehensive biomechanical study.[19]

Animal Model

The ovine tibia osteotomy model was used as it represents the most prevalent large animal model for evaluation of fracture healing.[20,22] The study was approved by the pertinent animal care committee and was consistent with previous studies on locking plate dynamization to facilitate comparability.[1,2,15] Twelve skeletally mature female Swiss Alpine sheep (2.6 $\pm$ 0.1 years old, 67 $\pm$ 8 kg weight) were randomized into the CP and ACTIVE groups. Under general anesthesia, an approximately 8-cm long medial incision was made over the tibia of one hind leg, whereby surgery was randomized between right and left hind legs. All 6 screw holes were drilled in the intact tibia with a custom drill template. A transverse osteotomy was performed with a 0.6-mm thick saw blade under constant irrigation. To ensure anatomic reduction, the distance between the central screw holes in plates was 0.6 mm shorter than in the drill template.

Osteotomies were stabilized with plates applied to the medial tibial shaft in a periosteum-sparing biological fixation technique to preserve periosteal perfusion.[23] In the CP group, plates were applied with 6 eccentrically inserted 4.5-mm cortical screws to achieve absolute stability and interfragmentary compression. In the ACTIVE group, plates were applied with six 5.0-mm bi-cortical locking screws to achieve direct apposition and dynamic stabilization. A standard postoperative medication protocol was followed.[22] Prophylactic antibiosis with benzylpenicillin and gentamicin, and analgesia with carprofen (4 mg/kg BW) and buprenorphine were initiated preoperatively and were continued for 4 days postoperatively. After surgery, a cylindrical cast was applied over a soft padding layer proximal to the hoof and extending to the knee joint. In the ovine osteotomy mode, this routine prophylactic measure is essential to prevent tibial fracture caused by bending loads while allowing axial load-bearing and ambulation immediately postsurgery.[1,2,15,17,24]

Planar Radiography

Radiographs were obtained immediately postoperative and in weekly intervals, starting at postoperative week 3 to quantify periosteal callus formation. At each timepoint, an anteroposterior radiograph and 2 lateral oblique radiographs ($\pm$10 degrees) were obtained to visualize the anterior, posterior, and lateral cortices without obstruction by the medially applied plate. Projected callus areas were measured using validated custom software developed to objectively quantify periosteal callus size.[25] This software used known plate dimensions as length standards for dimensional scaling. After automated demarcation of cortical boundaries, it derived consistent gray-scale thresholds for callus area extraction by accounting for cortex and background intensities.

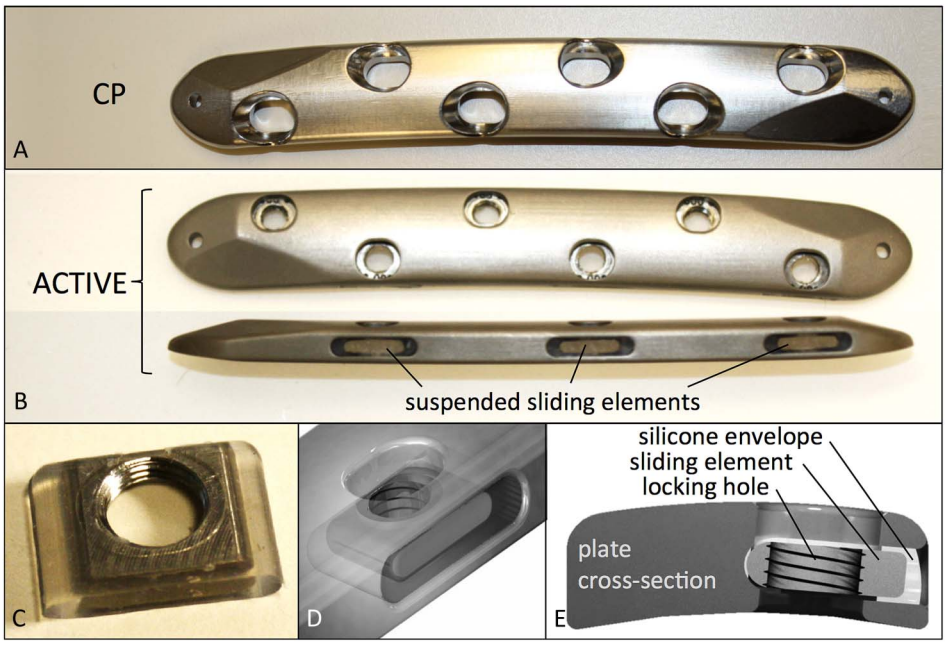

FIGURE 1. A, Standard CP. B, Dimensionally identical active plate with elastically suspended screw holes. C, Sliding element with locking hole, embedded in silicone envelope, and (D) inserted in lateral plate pocket. E, Cross-section of active plate.

Mechanical Testing

The proximal and distal ends of the tibiae were cemented in mounting fixtures that were separated by 170 mm and aligned with the tibial shaft axis. To ensure unconstrained torsion of the tibial shaft in a material test system (Instron 8874, High Wycombe, United Kingdom), the distal fixture was mounted on an x-y table that enabled translation but prevented rotation of the distal fixture around the diaphyseal axis. After implant removal, rotation was applied proximally at 10 degrees/minute to induce quasi-static loading until specimen failure in torsion.[1,2] Failure was defined as the instant at which rotational displacement caused a decrease in torsional moment due to specimen fracture or shearing at the osteotomy. At the instant of failure, the peak torque and rotation to failure were extracted from the torsion and rotation data, respectively. The strength of healed tibiae was quantified by the energy to failure, calculated by integrating the area under the torsion versus rotation curve up to the peak torque at which failure occurred.[1,2] The strength of the healed tibiae was furthermore normalized and expressed as a percentage of the native strength of the contralateral tibiae.

Computed Tomography

After torsion testing to failure, CT reconstructions of each specimen were obtained to identify the failure mode and to visualize the fracture pattern. Furthermore, transverse cross-sections adjacent to the osteotomy site were extracted to visualize the extent of circumferential callus formation. Finally, the osteotomy zone of one representative specimen of each group was analyzed using a μCT (80; Scanco Medical AG, Brüttisellen, Switzerland) with 5-μm spatial resolution to visualize fracture healing in anteroposterior and transverse cross-sectional views.

Statistical Analysis

All data are reported as the mean and SD. Sheep weight and age, and the outcome parameters callus area, peak torque, rotation to failure, and energy to failure were statistically compared between the CP and ACTIVE groups. In addition, these outcome parameters were statistically compared for the native contralateral tibiae to determine similarity of sheep in both groups. Statistical differences were tested using 2-tailed, unpaired Student *t* tests at a level of significance of $\alpha = 0.05$.

RESULTS

All sheep tolerated the experimental procedure without complications, were able to walk on postoperative day 1, and retained stable fixation of the tibial osteotomy until their sacrifice at week 9.

Radiographic Assessment

Healing in both groups resulted in periosteal callus formation in every specimen (see **Figure, Supplemental Content 1A**, http://links.lww.com/BOT/A818). At the earliest timepoint (week 3), the callus area in the ACTIVE group (235 ± 172 mm^2) was over 3 times greater than in the CP group (70 ± 31 mm^2, $P = 0.043$) (see **Figure, Supplemental Content 1B**, http://links.lww.com/BOT/A818). After week 6, the periosteal callus area decreased in both groups as a typical sign of remodeling. By week 9, the callus area in the ACTIVE group (451 ± 118 mm^2) remained almost 6 times greater than in the CP group (76 ± 16 mm^2, $P < 0.001$). Week 9 radiographs, obtained after sacrifice and resection of the soft tissue envelope, provided the clearest visualization of the fracture healing mechanism (Fig. 2). All ACTIVE specimens healed by secondary bone healing with abundant callus formation. No CP specimen demonstrated the abundant callus formation characteristic for secondary bone healing. Conversely, no CP specimen demonstrated purely primary bone healing without periosteal callus formation.

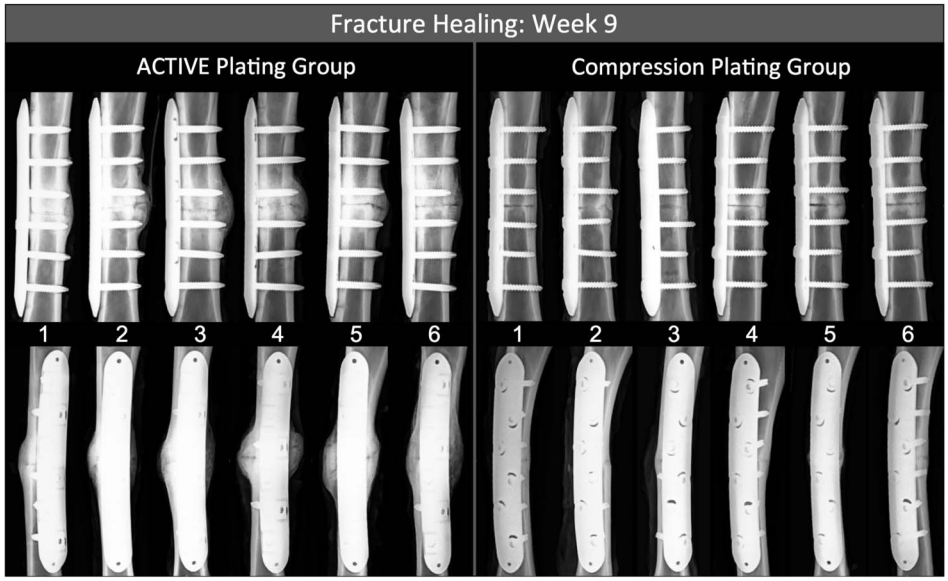

FIGURE 2. Final radiographs of the 6 specimens from both groups, obtained after sacrifice 9 weeks postsurgery. Periosteal callus was visible in all specimens. ACTIVE specimens demonstrated the classical mechanism of biologic bone healing by robust callus formation and bridging. Compression plating suppressed callus formation to a large degree.

Mechanical Testing

Torsion testing after implant removal demonstrated that ACTIVE specimens healed significantly stronger than specimens of the CP group (Table 1). ACTIVE specimens sustained a 35% greater peak torque ($P = 0.033$) and a 65% higher rotation to failure ($P = 0.009$) than CP specimens. The strength of ACTIVE specimens, expressed in terms of the energy required to induce failure, was 147% greater than in CP specimens ($P = 0.023$). Compared with contralateral intact tibiae, CP specimens had recovered on average 24% of their native strength, which was less than half of the 64% strength recovery obtained with ACTIVE specimens ($P = 0.008$) (see **Figure, Supplemental Content 2**, http://links.lww.com/BOT/A819). Comparison of contralateral tibiae yielded no significant differences between groups in peak torque ($P = 0.17$), rotation to failure ($P = 0.99$), and energy to failure ($P = 0.49$), demonstrating that the native tibiae in the CP and ACTIVE groups were statistically similar.

CT Analysis

Three of the 6 ACTIVE specimens (1, 5, and 6) failed outside the callus zone by spiral fracture through a screw hole (Fig. 3). All 6 CP specimens failed partially through the osteotomy in a bi-modal pattern, which involved a transverse fracture line through a portion of the transverse osteotomy that transitioned into an oblique fracture line through the remainder of the cortex. Transverse CT slices extracted adjacent to the osteotomy demonstrated that CP constructs healed with little and inconsistent periosteal callus that extended along a portion of the circumference. In contrast, each ACTIVE specimen developed circumferential callus that circumscribed the lateral, anterior, and posterior cortices, and traced the plate medially. Despite this circumferential callus, active plates did not adhere to the callus and could be removed with minimal effort because a thin fibrous sheath formed between the plate and callus in every ACTIVE specimen.

μCT imaging of a representative specimen of each group (Fig. 4A) revealed distinct and divergent fracture healing mechanisms. The CP specimen healed with 2 distinct mechanisms: localized direct bony union with minimal callus formation at one cortex, and gap healing with transversely arranged trabeculae at the opposing cortex. Conversely, the ACTIVE specimen demonstrated the classical mechanisms of secondary bone healing, where periosteal and endosteal callus bridged the osteotomy, while the osteotomy surface underwent resorption and showed no signs of direct bony healing (Fig. 4B). Transverse cross-sections adjacent to the osteotomy of the CP and ACTIVE specimens demonstrated porosis and progressive resorption of the cortical boundaries, indicative of cortical remodeling (Fig. 4C). Spatial reconstruction of μCT images confirmed the bi-modal fracture pattern of CP specimens (Fig. 4D), whereby a transverse fracture line traced the osteotomy segment that underwent gap healing, and propagated obliquely through the remaining cortex that presented signs of remodeling-induced cortical resorption.

DISCUSSION

Results of this in vivo study confirmed the hypothesis that dynamic stabilization with active locking plates delivers stronger healing of an anatomically reduced osteotomy compared with standard compression plating in a controlled ovine fracture healing model.

The theory of primary bone healing commands 2 stringent prerequisites: direct bony apposition and absolute stability.[21,26] Results of the CP group demonstrated that these prerequisites are difficult to achieve at best, even in the presence of strong bone, a simple osteotomy, and joint execution of osteosynthesis by an experienced orthopedic surgeon (SM) and a seasoned veterinary surgeon (BvR) with extensive training by the Arbeitsgemeinschaft für Osteosynthesefragen (AO). The presence of small amounts of periosteal callus indicated that absolute stability was not achieved in the CP

TABLE 1. Comparison of Outcome Parameters Between CP and ACTIVE Groups

	CP Group	ACTIVE Group	% Difference	*P*
Sheep weight, age				
Weight, kg	68 (8)	67 (7)	2	0.80
Age, mo	30 (0.4)	31 (0.8)	3	0.26
Periosteal callus area (anterior, posterior, and lateral aspects), mm^2				
Week 3 postop	70 (31)	235 (172)	236	0.043
Week 9 postop	76 (16)	451 (118)	493	<0.001
Mechanical properties (absolute)				
Peak torque, Nm	43 (8)	58 (12)	35	0.033
Rotation to failure, degree	7.8 (2.0)	12.9 (3.4)	65	0.009
Energy to failure, Nm·degree	193 (95)	476 (240)	147	0.023
Mechanical properties (normalized)				
Peak torque (% of contralateral)	51 (11)	75 (17)	47	0.017
Rotation to failure (% of contralateral)	45 (13)	75 (16)	67	0.006
Energy to failure (% of contralateral)	24 (13)	64 (27)	167	0.008
Mechanical properties (contralateral tibiae of CP and ACTIVE groups, provided for reference only)				
Peak torque, Nm	84 (8)	78 (7)	7	0.17
Rotation to failure, degree	17.2 (2.9)	17.2 (1.7)	0	0.997
Energy to failure, Nm·degree	798 (178)	741 (90)	7	0.49

group. Gap healing indicated deficient bony apposition at a portion of the osteotomy surface. Our findings directly correlate to the original description of direct bone healing by Perren et al[26] in 1967, which used the same ovine tibia transverse osteotomy model. Despite using 2 plates placed at right angles, they only observed primary bone healing at the cortical aspect between the 2 plates. Similar to our findings, they noted lamellar bone in the form of transverse osteons at the opposite cortex. Most recently, Plecko et al[27] evaluated healing of oblique osteotomies in the ovine tibia model. Despite using an interfragmentary lag screw or locking screws to supplement compression plating, they still observed 4–5 mm thick periosteal callus at the far cortex. This published evidence concurs with the findings of this study that compression plating may not yield purely primary bone healing. Instead, compression plating leads to a combination of primary healing, gap healing, minimal periosteal callus formation, and cortical porosis. This observation is consistent with the clinical experience that compression plating is technically demanding, and primary bone healing is at best difficult to obtain.[8,10,12] In stark contrast, active plates supported natural bone healing by early, abundant, and circumferential callus formation. This robust healing response relied entirely on periosteal and endosteal callus formation, without any form of healing between adjacent osteotomy surfaces. Instead, osteotomy surfaces resorbed as part of the global remodeling process.

This natural bone healing of simple, well-reduced fractures under conditions of dynamic stabilization has previously been documented using sliding plates[7] and axially flexible plates,[4,8] and is routinely anticipated with intramedullary nailing. The concept of dynamic stabilization of simple fractures with plates has been proposed as early as 1943 in the form of a 2-part sliding plate to ensure bony apposition and dynamic loading at the fracture site.[28] In 1999, this 2-part sliding plate design was evaluated in vivo and delivered faster callus maturation and healing than absolute stabilization with standard compression plating.[7] Likewise, Foux et al[4] tested nonlocking axially flexible plate designs that used sliding inserts. Their axially flexible plates also demonstrated superior healing of simple, well-reduced fractures compared with absolute stabilization with CPs. Most recently, dynamization of locking plates with dynamic locking screws (Synthes, Solothurn, Switzerland) was evaluated for stabilization of an anatomically reduced oblique osteotomy of the ovine tibia in the absence and presence of a fracture gap.[24] Similar to this study, they found that even in the absence of a fracture gap, dynamic stabilization yielded strong periosteal callus formation and remodeling of osteotomy surfaces, but they did not report the strength of healed tibiae.

This study quantified that by week 9, active plates restored on average 64% of the native tibial strength, whereas compression plating restored only 24% of native strength. Clinically, this early strength recovery is critical for timely return to function and for mitigation of fixation failure. Most interestingly, a previous study demonstrated that bridging a 3-mm osteotomy gap with an active plate restored on average 81% of the native tibial strength by week 9.[2] This superior healing compared with this study may be attributed to the enhanced axial dynamization permitted by a fracture gap. Clinically, this would imply that active plates facilitate biological plating strategies in which functional alignment and soft tissue preservation is favored over anatomic reduction and fracture compression. Based on the relative ease of implantation, intramedullary nailing has largely replaced compression plating in the treatment of long bone fractures. Active plating mimics intramedullary nailing, a more forgiving osteosynthesis strategy that reliably supports natural bone healing with periosteal callus formation in simple and comminuted fractures with less stringent reduction and stabilization requirements. Active plating also preserved the intramedullary canal and yielded endosteal callus formation.

These results are specific to the ovine osteotomy model and therefore require careful interpretation before extrapolation to clinical practice. The ovine model represents the gold standard fracture healing model in large animals[20,22] that has been consistently used since Perren et al explored primary bone healing.[26] Load transmission in the ovine tibia

FIGURE 3. CT analysis after fracture due to mechanical testing: Three of the 6 ACTIVE specimens failed by spiral fracture through a screw hole outside the callus zone. All 6 CP specimens failed partially through the osteotomy. Transverse CT slices extracted adjacent to the osteotomy, rotated to depict the plate to the left side, demonstrated circumferential periosteal callus in all ACTIVE specimens, and severely suppressed callus in CP specimens.

corresponds in magnitude to lower extremity loading in humans.[29] Despite evidence from this well-established fracture healing model that active plating can deliver stronger healing of simple fractures, a well-designed prospective clinical trial will be required to assess if active plating can reduce healing complications and can facilitate an earlier return to function.

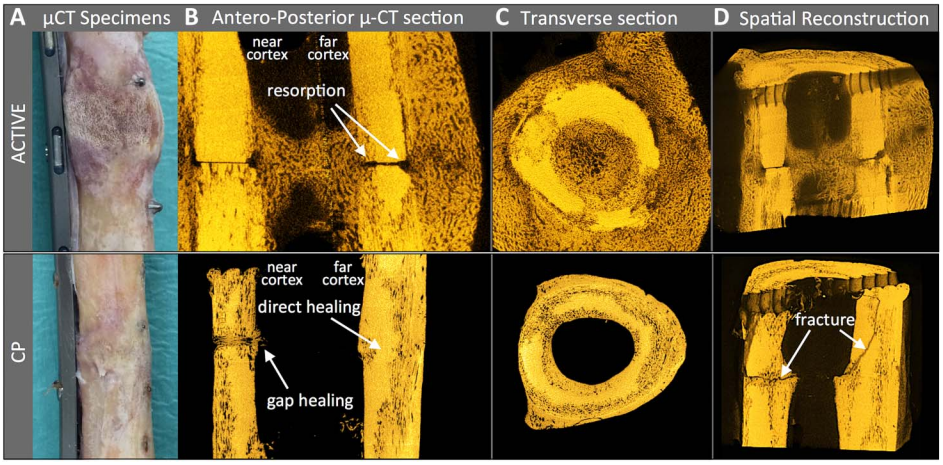

FIGURE 4. μCT analysis after fracture due to mechanical testing: (A) Photograph of one representative specimen of each group. B, The ACTIVE specimen depicts periosteal and endosteal callus, and resorption of the osteosynthesis surface. The CP specimen depicts gap healing with transverse osteons on the plate side, and direct, primary bone healing at the far cortex. C, Transverse cross-sections adjacent to the osteotomy show cortical resorption in both specimens. D, The CP specimen illustrates a transverse fracture line through a gap-healing zone, that extends into an oblique fracture through the opposite cortex which healed by primary one healing.

In conclusion, findings of this study provided further evidence that achieving primary bone healing by compression plating is difficult to achieve and may include gap healing with some periosteal callus formation due to deficient stability and bony apposition. Compared with compression plating, active plating delivered stronger healing of simple fractures, whereby active plating specimens healed to be over twice as strong by week 9. In combination, these findings challenge the currently accepted axiom of compression plating for simple fracture patterns.

REFERENCES

1. Bottlang M, Lesser M, Koerber J, et al. Far cortical locking can improve healing of fractures stabilized with locking plates. *J Bone Joint Surg Am.* 2010;92:1652–1660.
2. Bottlang M, Tsai S, Bliven EK, et al. Dynamic stabilization with active locking plates delivers faster, stronger, and more symmetric fracture-healing. *J Bone Joint Surg Am.* 2016;98:466–474.
3. Claes L. Biomechanical principles and mechanobiologic aspects of flexible and locked plating. *J Orthop Trauma.* 2011;25(suppl 1):S4–S7.
4. Foux A, Yeadon AJ, Uhthoff HK. Improved fracture healing with less rigid plates. A biomechanical study in dogs. *Clin Orthop Rel Res.* 1997; 339:232–245.
5. Goodship AE, Kenwright J. The influence of induced micromovement upon the healing of experimental tibial fractures. *J Bone Joint Surg Am.* 1985;67:650–655.
6. Kenwright J, Richardson JB, Cunningham JL, et al. Axial movement and tibial fractures. A controlled randomised trial of treatment. *J Bone Joint Surg Am.* 1991;73:654–659.
7. Panagiotopoulos E, Fortis AP, Lambiris E, et al. Rigid or sliding plate. A mechanical evaluation of osteotomy fixation in sheep. *Clin Orthop Rel Res.* 1999;358:244–249.
8. Uhthoff HK, Poitras P, Backman DS. Internal plate fixation of fractures: short history and recent developments. *J Orthop Sci.* 2006;11:118–126.
9. Lujan TJ, Henderson CE, Madey SM, et al. Locked plating of distal femur fractures leads to inconsistent and asymmetric callus formation. *J Orthop Trauma.* 2010;24:156–162.
10. Rahn BA, Gallinaro P, Baltensperger A, et al. Primary bone healing. An experimental study in the rabbit. *J Bone Joint Surg Am.* 1971;53:783–786.
11. Roderer G, Gebhard F, Duerselen L, et al. Delayed bone healing following high tibial osteotomy related to increased implant stiffness in locked plating. *Injury*. 2014;45:1648–1652.
12. Woo SL, Lothringer KS, Akeson WH, et al. Less rigid internal fixation plates: historical perspectives and new concepts. *J Orthop Res.* 1984;1:431–449.
13. Adams JD, Jr, Tanner SL, Jeray KJ. Far cortical locking screws in distal femur fractures. *Orthopedics*. 2015;38:e153–e156.
14. Bottlang M, Fitzpatrick DC, Sheerin D, et al. Dynamic fixation of distal femur fractures using far cortical locking screws: a prospective observational study. *J Orthop Trauma.* 2014;28:181–188.
15. Dobele S, Gardner M, Schroter S, et al. DLS 5.0–the biomechanical effects of dynamic locking screws. *PLoS One*. 2014;9:e91933.
16. Freude T, Schroter S, Gonser CE, et al. Controlled dynamic stability as the next step in "biologic plate osteosynthesis"—a pilot prospective observational cohort study in 34 patients with distal tibia fractures. *Patient Saf Surg.* 2014;8:3.
17. Richter H, Plecko M, Andermatt D, et al. Dynamization at the near cortex in locking plate osteosynthesis by means of dynamic locking screws: an experimental study of transverse tibial osteotomies in sheep. *J Bone Joint Surg Am.* 2015;97:208–215.
18. Capanni F, Hansen K, Fitzpatrick DC, et al. Elastically suspending the screw holes of a locked osteosynthesis plate can dampen impact loads. *J Appl Biomech.* 2015;31:164–169.
19. Tsai S, Fitzpatrick DC, Madey SM, et al. Dynamic locking plates provide symmetric axial dynamization to stimulate fracture healing. *J Orthop Res.* 2015;33:1218–1225.
20. Nunamaker DM. Experimental models of fracture repair. *Clin Orthop Rel Res.* 1998;355(suppl):S56–S65.
21. Perren SM. The concept of biological plating using the limited contact-dynamic compression plate (LC-DCP). Scientific background, design and application. *Injury*. 1991;22(suppl 1):1–41.
22. Auer JA, Goodship A, Arnoczky S, et al. Refining animal models in fracture research: seeking consensus in optimising both animal welfare and scientific validity for appropriate biomedical use. *BMC Musculoskelet Disord.* 2007;8:72.
23. Perren SM. Evolution of the internal fixation of long bone fractures. The scientific basis of biological internal fixation: choosing a new balance between stability and biology. *J Bone Joint Surg Am.* 2002; 84:1093–1110.
24. Plecko M, Lagerpusch N, Andermatt D, et al. The dynamisation of locking plate osteosynthesis by means of dynamic locking screws (DLS)-an experimental study in sheep. *Injury*. 2013;44: 1346–1357.
25. Lujan TJ, Madey SM, Fitzpatrick DC, et al. A computational technique to measure fracture callus in radiographs. *J Biomech.* 2010;43: 792–795.
26. Perren SM, Huggler A, Russenberger M, et al. The reaction of cortical bone to compression. *Acta Orthop Scan Suppl.* 1969;125:19–29.
27. Plecko M, Lagerpusch N, Pegel B, et al. The influence of different osteosynthesis configurations with locking compression plates (LCP) on stability and fracture healing after an oblique 45 degrees angle osteotomy. *Injury*. 2012;43:1041–1051.
28. Longfellow EE, inventors; Surgical appliance for bone fracture. assignee. US Patent and Trademark Office, patent number 2,486,303, 1949.
29. Taylor WR, Ehrig RM, Heller MO, et al. Tibio-femoral joint contact forces in sheep. *J Biomech.* 2006;39:791–798.